Earth System
Dynamics
Discussions

Different response of surface temperature and air temperature to deforestation in climate models

Johannes Winckler[1,2,3], Christian H. Reick[1], Sebastiaan Luyssaert[4], Alessandro Cescatti[5], Paul C. Stoy[6], Quentin Lejeune[7,8], Thomas Raddatz[1], Andreas Chlond[1], Marvin Heidkamp[1,2], and Julia Pongratz[1,9]

[1]Max Planck Institute for Meteorology, Hamburg, Germany.
[2]International Max Planck Research School on Earth System Modeling, Hamburg, Germany.
[3]Current affiliation: Laboratoire des Sciences du Climat et de l'Environnement, LSCE/IPSL, CEA-CNRS-UVSQ, Université Paris-Saclay, 91191 Gif-sur-Yvette, France.
[4]Vrije Universiteit Amsterdam, Faculty of Science, 1081 HV, the Netherlands.
[5]European Commission, Joint Research Centre, Institute for Environment and Sustainability, Ispra, Italy.
[6]Department of Land Resources and Environmental Sciences, Montana State University, Bozeman, MT, USA.
[7]Institute for Atmospheric and Climate Science, ETH-Zürich, Switzerland.
[8]Current affiliation: Climate Analytics, Berlin, Germany.
[9]Current affiliation: Ludwig-Maximilians-Universität München, Munich, Germany.

Correspondence: Johannes Winckler(johannes.winckler@lsce.ipsl.fr)

Abstract. Deforestation affects temperatures at the land surface and higher up in the atmosphere. Satellite-based observations typically register deforestation-induced changes in surface temperature, in-situ observations register changes in near-surface air temperature, and climate models simulate changes in both temperatures and the temperature of the lowest atmospheric layer. Yet a focused analysis of how these variables respond differently to deforestation is missing. Here, this is investigated by

5 analyzing the biogeophysical temperature effects of large-scale deforestation in the climate model MPI-ESM, separately for local effects (which are only apparent at the location of deforestation) and nonlocal effects (which are also apparent elsewhere). While the nonlocal effects affect the temperature of the surface and lowest atmospheric layer equally, the local effects mainly affect the temperature of the surface. In agreement with observation-based studies, the local effects on surface and near-surface air temperature respond differently in the MPI-ESM, both concerning the magnitude of local temperature changes and the

10 latitude at which the local deforestation effects turn from a cooling to a warming (at 45-55° N for surface temperature and around 35° N for near-surface air temperature). An inter-model comparison shows that in the northern mid latitudes, both for summer and winter, near-surface air temperature is affected by the local effects only about half as much compared to surface temperature. Thus, studies about the biogeophysical effects of deforestation must carefully choose which temperature they consider.

15   1   Introduction

Afforestation has been proposed as a tool to mitigate climate change globally (UNFCCC, 2011), mainly because forests can store large amounts of carbon (Luyssaert et al., 2008; Le Quéré et al., 2017). Much less considered are the climate changes, be it cooling or warming, that are caused by changes in forest cover via an alteration of the exchange of energy and water

between the Earth's surface and the atmosphere, i.e. the so-called biogeophysical effects (Bonan, 2008). Earth System models have been employed to assess how these biogeophysical effects affect the temperature of the *surface* (e.g., Bala et al., 2007; Pongratz et al., 2010; Davin and de Noblet-Ducoudre, 2010; Boisier et al., 2012; Devaraju et al., 2015; Li et al., 2016) and the temperature of the *near-surface air* (usually air at 2 m) (e.g., Claussen et al., 2001; Gibbard et al., 2005; Findell et al., 2006; Pitman et al., 2009; Bathiany et al., 2010; de Noblet-Ducoudré et al., 2012; Jones et al., 2013). Surface temperature matters for habitat and vegetative function (e.g., Chen et al., 1999; De Frenne et al., 2013) while near-surface air temperature is often considered to be more related to the temperature that humans perceive (e.g., Staiger et al., 2011). The focus of this study is the question whether surface temperature and near-surface air temperature respond differently to deforestation in climate models.

An answer to this question could help to reconcile apparent inconsistencies in observation-based studies on the effects of deforestation on surface temperature and air temperature. Studies based on satellite observations (Li et al., 2015; Alkama and Cescatti, 2016; Duveiller et al., 2018) investigated changes in radiometric surface temperature which, with its heterogeneous emissivity (Jin and Dickinson, 2010), represents a combination of temperature of the vegetation and the soil (through gaps in the canopy). The studies based on satellite observations reported that deforestation leads to a local cooling in the boreal regions (north of approx. 45-55°N) and a warming in lower latitudes. Studies based on observations of air temperature from weather stations and Fluxnet towers (Lee et al., 2011; Zhang et al., 2014) also reported a deforestation-induced boreal local cooling and a warming for lower latitudes, but they indicated that the transition between cooling and warming is located further south (at approx. 35°N). It remains unclear whether part of this apparent inconsistency can be attributed to the different heights at which temperature changes are considered. In contrast to the observations, climate models allow us to assess the biogeophysical effects both on surface temperature, on near-surface air temperature, and temperature of the atmosphere within one consistent framework, and thus climate models are suitable to investigate this question.

Both the air and surface temperature can be influenced by local and nonlocal biogeophysical effects of deforestation. We define local effects as effects that are only apparent in deforested locations and nonlocal effects as effects that are also apparent in non-deforested locations (Methods and Winckler et al., 2017). Local effects can for example be caused by a redistribution of heat between the surface and the atmosphere (e.g., Vanden Broucke et al., 2015) while the nonlocal effects can be caused by changes in global circulation (Swann et al., 2012; Devaraju et al., 2015; Lague and Swann, 2016) or advection (Winckler et al., 2018). Here, we consider local and nonlocal effects separately for three reasons. First, the difference between local and nonlocal effects matters for decision makers: the local effects may be relevant for policies that aim at adapting to a warming climate locally because they link the climate effects to the areas where policies are implemented (Duveiller et al., 2018). The nonlocal effects are also relevant for international policies that aim at mitigating global climate change because the nonlocal effects may dominate the global mean biogeophysical temperature response to deforestation (Winckler et al., 2018). Second, the observation-based data-sets only record the local effects when comparing nearby locations with and without deforestation. The nearby locations share the same background climate, and thus the nonlocal effects cancel out when temperature differences between the locations are considered (Lee et al., 2011; Li et al., 2015; Alkama and Cescatti, 2016; Duveiller et al., 2018). For a consistent comparison to observation-based data-sets, the local effects have to be isolated from the climate model results. The third reason to consider local and nonlocal temperature changes separately is that different mechanisms trigger local and

nonlocal temperature changes (Winckler et al., 2017). If surface and air temperature respond differently to deforestation, it is unclear whether this difference arises from the mechanisms that trigger the local temperature changes, the mechanisms that trigger the nonlocal temperature changes, or both. A separate analysis of local and nonlocal temperature changes facilitates an investigation of the mechanisms that may cause a different response of surface and air temperature to deforestation.

5   Here, we investigate how deforestation in the MPI-ESM climate model affects surface and air temperature differently and analyze this separately for the local and nonlocal effects. Thus, we emulate the deforestation effects on surface temperature as estimated from satellite data and near-surface air temperature as estimated from in-situ measurements within a consistent framework. In a previous study it was noted that surface and air temperature response differ mainly for the local effects (Appendix C in Winckler et al., 2017). We go beyond this previous study by using simulations with an interactive ocean because

10   this is essential to capture the full climate effects of deforestation (Davin and de Noblet-Ducoudre, 2010). This previous study (Winckler et al., 2017) contrasted the response of surface temperature only with the response of near-surface air temperature, while here we additionally analyze the effects on temperature in the lowest atmospheric layer. To further analyze the mechanisms that are responsible for differences in these three temperature variables, we investigate the local effects separately for the response in mean daily minimum and maximum temperature. To test the robustness of our results for this particular climate

15   model, we contrast the response of the local effects on near-surface air temperature and surface temperature across a wide range of climate models.

2   Methods

2.1   Simulations of large-scale deforestation in the MPI-ESM

Using the fully coupled climate model MPI-ESM (Giorgetta et al., 2013), the temperature response to deforestation at the

20   surface, at 2 m and the lowest layer of the atmosphere are obtained from simulations of large-scale deforestation. 550 years of simulations are performed in T63 atmospheric resolution (about 1.9°) and the last 200 years (which are free of substantial trends in the investigated variables (not shown)) are used for the analysis. Following the approach as in a previous study (Winckler et al., 2017), two simulations are performed: a first simulation ('forest world') with forest plant functional types on all areas where vegetation is present at pre-industrial times (i.e. forests do not exist in deserts etc.). These vegetated areas from a

25   previous study (Pongratz et al., 2008) were reconstructed from potential vegetation based on remote sensing data (Ramankutty and Foley, 1999). In a second simulation forests are completely replaced by grasslands in three of four grid boxes in a regular spatial pattern (equivalent to simulation '3/4' in a previous study (Winckler et al., 2018)). In both simulations, atmospheric CO_2 concentrations are prescribed at pre-industrial level in order to obtain only the biogeophysical effects of deforestation. The total (local plus nonlocal) biogeophysical deforestation effects are then computed as the differences (e.g., in temperature)

30   between these two simulations.

Following the approach in Winckler et al. (2017), the total effects can be separated into the local and nonlocal effects of deforestation as follows:

$$\Delta T^{total} = \Delta T^{local} + \Delta T^{nonlocal} + \Delta T^{(local \times nonlocal)},$$

where ΔT^{total} are the temperature changes that are simulated at a deforested grid box and $\Delta T^{(local \times nonlocal)}$ are possible interactions between local and nonlocal effects. We neglect these interactions here because they were found to be small for a wide range of deforestation scenarios (Winckler et al., 2017). The nonlocal effects are determined from non-deforested grid boxes, where only the nonlocal effects are present. The nonlocal effects are spatially interpolated to the deforested grid boxes. The local effects at deforested grid boxes can thus be obtained by subtracting the nonlocal effects from the simulated total effects:

$$\Delta T^{local} = \Delta T^{total} - \Delta T^{nonlocal}.$$

The local effects are thus the temperature changes that exceed the nonlocal temperature changes that are obtained by interpolation from nearby non-deforested grid boxes. A detailed description of the separation approach can be found in Winckler et al. (2017).

2.2 Temperature of the surface, the lowest atmospheric layer, and near-surface air in the MPI-ESM

5   This study investigates the response of three types of temperature to deforestation in the MPI-ESM: surface temperature (T_{surf}), temperature of the lowest atmospheric layer (T_{atm}, in the following 'atmospheric temperature'), and near-surface air temperature (T_{2m}, called 'tas' in the Climate Model Intercomparison Project CMIP5 and in the following 'air temperature'). These temperature variables are part of the standard output of climate model simulations. In the following, we describe how their values are obtained in the MPI-ESM.

10   The surface temperature T_{surf} in the MPI-ESM is determined by solving the surface energy balance equation in a bulk canopy layer. For simplicity this layer has a heat capacity that is independent of the vegetation type. This bulk canopy layer exchanges heat with deeper soil layers via the ground heat flux.

    It is not possible to assign one geometrical height to the surface layer in the MPI-ESM because there is an internal inconsistency between the two different aspects that are involved in the process of solving the surface energy balance equation: the
15 calculation of the surface radiative budget (absorption of solar radiation and emission of terrestrial radiation to the atmosphere) and the calculation of the turbulent heat fluxes (latent and sensible heat). From the perspective of the radiative budget, the surface is where this radiative budget is calculated (i.e. where the energy balance is solved). In the presence of vegetation this is somewhere in the canopy, but geometrically its exact height cannot be specified. From the perspective of turbulent fluxes, the geometrical height $d + z_0$ above the surface is where the wind speed would become zero in the wind profile based on
20 Monin-Obukhov theory (Leclerc and Foken, 2014). Here, z denotes the height above the ground and d is the zero-plane displacement height. This d takes into account the displacement effect exerted by vegetation (Leclerc and Foken, 2014; Campbell and Norman, 1998). Geometrically the height $d + z_0$ may differ from the height where the radiative budget is calculated.

What does this inconsistency imply for the comparison between T_{surf} in the MPI-ESM and satellite-based products? For comparison with satellite observations only the radiative perspective is relevant – because satellites estimate temperature based on the emissions of terrestrial radiation. That the Monin-Obukhov theory provides a different definition of surface height must be considered as a special approximation to solve the energy balance, but has no consequences for comparison with satellite observations of surface temperature.

The 'atmospheric temperature' T_{atm} is defined here as the temperature of the lowest of the 47 atmospheric layers in the MPI-ESM (Stevens et al., 2013). The thickness of this layer is around $60\,m$ (at $15°C$), and the temperature is volume-averaged in this layer. This temperature is used for the calculation of the turbulent heat fluxes and T_{surf}.

The near-surface air temperature T_{2m} is estimated in the MPI-ESM as the air temperature $2\,m$ above $d + z_0$. Because it is unclear (and irrelevant for the calculations) where within the canopy this $d + z_0$ is, a comparison of T_{2m} between the MPI-ESM and observations is challenging, especially in forests (see Discussions). The MPI-ESM does not have a representation of within-canopy air temperature or separate temperatures of the surface and the vegetation canopy.

In the MPI-ESM, T_{2m} is obtained via a procedure based on Monin-Obukhov similarity theory that uses the values at the surface and the lowest atmospheric layer. This procedure employs dry static energy instead of temperature because dry static energy is a conserved quantity in an adiabatic process.

$$s_{z_{aero}} = c_p \cdot T_{z_{aero}} + g \cdot z_{aero}, \tag{1}$$

where $s_{z_{aero}}$ and $T_{z_{aero}}$ are the dry static energy and temperature at the aerodynamic height $z_{aero} = z - d$, c_p is the heat capacity of moist air, and g is the gravitational acceleration of the Earth.

At $2\,m$ above $d + z_0$, the dry static energy is then obtained as follows:

$$s_{2m} = s_{surf} + (s_{atm} - s_{surf})\gamma\left(\frac{2\,\text{m}}{z_0}, R_i\right), \tag{2}$$

where γ is a nonlinear function with values ranging between 0 and 1 that depends on the roughness length z_0 and on the bulk Richardson number R_i, which is closely related to the temperature gradient T_{surf}-T_{atm}. Different functions γ are used for near-surface neutral ($R_i \approx 0$), stable ($R_i < 0$), and unstable conditions ($R_i > 0$) (ECMWF Research Department, 1991, section 3.1.3). Note that both s_{surf} and s_{atm}, but also R_i and z_0 are affected by deforestation. After this procedure, T_{2m} is derived from s_{2m} using equation 1.

2.3 Isolation of local effects across models

In order to compare the results for the MPI-ESM with other climate models, the temperature response of and near-surface air and surface temperature to deforestation in the northern-hemisphere mid latitudes are compared across a wide range of climate models from CMIP5. For this comparison, we focus on the local effects for three reasons: first, the local effects exhibit a better signal/noise ratio compared to the nonlocal effects (e.g., Lejeune et al., 2017). This is important because the climate variability can be large compared to the nonlocal effects for the short time spans (30 years) that are analyzed here (Winckler et al., 2018).

Furthermore, climate variability is especially large in the mid-latitudes (Deser et al., 2012) that are analyzed here. Second, the nonlocal effects cannot be isolated from the analyzed set of all-forcing simulations (see below). Third, the local effects at one location are largely independent of deforestation elsewhere (Winckler et al., 2017) while the nonlocal effects strongly depend on the areal extent and spatial distribution of deforestation (Winckler et al., 2018).

5   We do not isolate the local effects for these models the same way as described in section 2.1 because this approach would have required repeating these simulations for every model. Instead, we isolate the local effects of deforestation in the difference between 'historical' and 'piControl' simulations from CMIP5 (Taylor et al., 2012). The 'historical' simulations are subject to all forcings including changes in greenhouse gases and land use while the 'piControl' simulations are subject to constant boundary conditions and no forcings. To isolate the local effects of deforestation, we use a method that was already applied

10 and validated on these simulations (Lejeune et al., 2018). This method assumes that T_{surf} and T_{2m} in neighboring grid boxes can be affected differently by the local effects of deforestation, depending on the forest cover change in each grid box, whereas other climate forcings (like greenhouse gases, but also the nonlocal effects) influence neighboring grid boxes in a similar way. The local effects are extracted by fitting linear regressions between temporal changes in temperature and forest cover change within a spatially moving window encompassing 5x5 model grid boxes.

15 We consider here the difference between the last 30 years (1971-2000) of 'historical' simulations for which data in all models are available and 30 years of the pre-industrial control simulations (piControl), from which the temporal changes in both temperature variables and forest fraction since 1860 are computed. The 'historical' simulations consist of several ensemble members for each model, where each ensemble member experiences the same forcings but starts from different initial conditions. The moving-window method is applied to several combinations of ensemble members from the 'historical'

20 simulations and time slices from the 'piControl' simulations for each model, and the number of analyzed ensemble members is shown in Table S1.

3   Results

3.1   Different temperature response of surface and air temperature in the MPI-ESM

In the MPI-ESM, global-scale deforestation (in three of four grid boxes) triggers substantial nonlocal cooling in most regions

25 (Fig. 1). Deforestation makes the atmosphere cooler and drier (not shown), and this leads to a reduction of T_{surf} in many regions, mainly because of reduced longwave incoming radiation (Davin and de Noblet-Ducoudre, 2010; Winckler et al., 2018). The spatial pattern of these nonlocal effects is very similar for T_{surf}, T_{2m} and T_{atm}.

In contrast to the nonlocal effects, the local effects differ strongly between T_{surf}, T_{2m}, and T_{atm}. Deforestation strongly influences the local surface energy balance: the imposed changes in surface properties in the model (surface albedo, evapotran-

30 spirative efficiency and surface roughness) cause a surface warming for the local effects in most regions, except for the high northern latitudes where the local effects cause a surface cooling (Fig. 1). The changes in surface properties influence not only

Earth System
Dynamics
Discussions
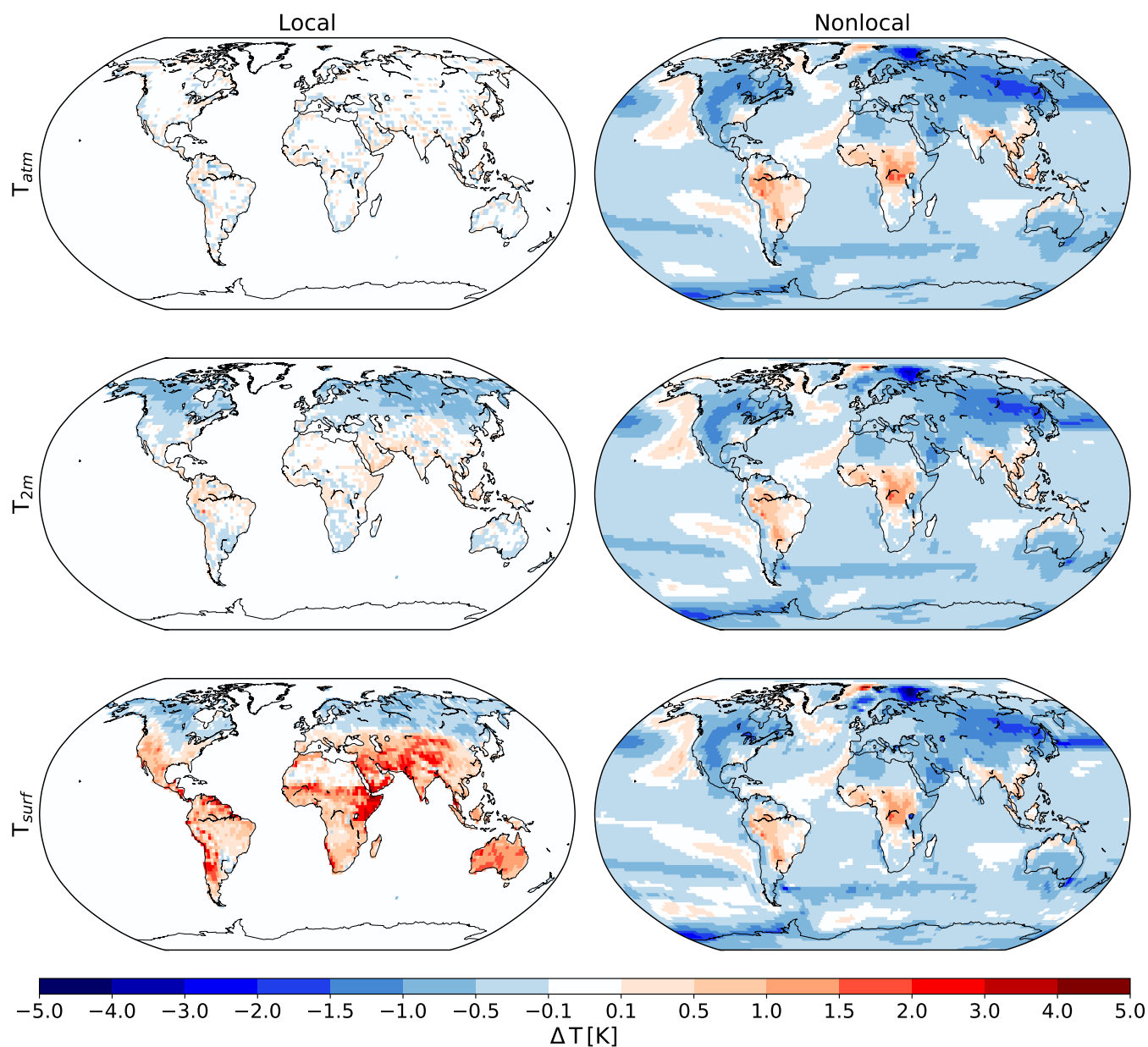
Figure 1. Response of temperature in the lowest atmospheric layer (T_{atm}), near-surface air (T_{2m}), and at the surface (T_{surf}) to deforestation.

the local surface temperature but also the flux of sensible heat from the surface into the lower boundary layer (not shown). Intuitively one would expect that the change in sensible heat flux alters T_{atm}, e.g. an increased input of sensible heat into the atmosphere could raise the temperature of the atmospheric air above a deforested location. However, in our model results T_{atm} is largely unaffected by the local effects of deforestation (Fig. 1). We interpret this lack of local effects in T_{atm} as follows:

the time needed for the lowest atmospheric layer to warm up due to the deforestation-induced increase in sensible heat flux is long enough for the heated air to be transported to higher atmospheric layers and the neighboring grid boxes. Due to the advection, the change in atmospheric temperature is hence not only seen in a deforested location but also in nearby grid boxes that are not deforested. Thus, this warming or cooling is accounted for in the nonlocal effects. In the nearby grid boxes, the

5 change in atmospheric temperature and/or moisture can then influence also T_{surf} via changes in longwave incoming radiation (Davin and de Noblet-Ducoudre, 2010; Winckler et al., 2018), which could explain why the nonlocal effects are similar for T_{atm} and T_{surf}. While in T_{atm}, advection can lead to a direct exchange of heat between neighboring grid cells, the same is not possible for T_{surf}; there is no direct horizontal exchange of heat between the surface of neighboring grid cells, and this difference (advection for T_{atm} but not T_{surf}) may explain why local effects can be seen in T_{surf} but not in T_{atm}.

10 Because the T_{2m} is an interpolation between T_{surf} and T_{atm}, we expected that also the local response of T_{2m} would lie in between the response of T_{surf} and T_{atm}. In a lot of regions this is the case, but in other regions, most notably those that show a cooling, the local effects on T_{2m} seem to cool more than T_{surf}, and in some regions even the sign differs between ΔT_{surf} and ΔT_{2m} (e.g. parts of the US and regions in the southern extra-tropics, Fig. S1). What the different response of T_{surf} and T_{2m} means in relation to the observation-based findings is discussed in section 4.

15 To understand the apparent discrepancy between ΔT_{surf} and ΔT_{2m}, we separately analyze the local temperature response for boreal winter (DJF) and summer (JJA), and the response of mean daily minimum temperature (T_{min}, which approximately corresponds to nighttime conditions) and maximum temperature (T_{max}, which approximately corresponds to daytime conditions). For surface temperature, the response to deforestation locally differs strongly between DJF, JJA, T_{min}, and T_{max} values (Fig. 2). The northern-hemisphere DJF and the T_{min} surface temperatures are strongly cooling for deforestation, while

20 the JJA and T_{max} surface temperatures are warming. This is qualitatively in good agreement with observation-based studies that show a local cooling in the boreal regions in DJF (Alkama and Cescatti, 2016; Bright et al., 2017; Duveiller et al., 2018) and in agreement with the local increase in the diurnal amplitude due to deforestation (Li et al., 2015; Alkama and Cescatti, 2016; Schultz et al., 2017). Similarly as in the case of long-term mean temperature (Fig. 1), T_{atm} locally hardly responds to deforestation, neither for DJF, JJA, T_{min}, nor T_{max}.

25 For near-surface air temperature, the T_{max} response is substantially weaker, and in many areas of opposite sign, than for the surface, similar to the lowest atmospheric layer (land mean absolute changes for T_{max}: 1.62 K for the surface, 0.19 K for near-surface air, and 0.10 K for the lowest atmospheric layer). On the contrary, most regions exhibit a strong T_{min} cooling of near-surface air temperature, similar to the T_{min} response of surface temperature (land mean absolute changes for T_{min}: 0.67 K for the surface, 0.48 K for the near-surface air, and 0.10 K for the lowest atmospheric layer). We interpret this as

30 follows: During daytime (during which T_{max} occurs), the surface temperature is higher than the temperature of the lowest atmospheric layer (Fig. S2), which means that near-surface atmospheric conditions are unstable. Deforestation reduces the roughness length z_0 and increases surface temperature (Fig. 1) and thus also atmospheric instability (illustrated in Figure S3 b), and this influences the Richardson number R_i which enters the Monin-Obukhov function for near-surface air temperature (γ in equation 2, see underlying report (ECMWF Research Department, 1991)) such that near-surface air temperature in the

35 model may decrease although surface temperature increases. During nighttime (during which T_{min} occurs), the near-surface
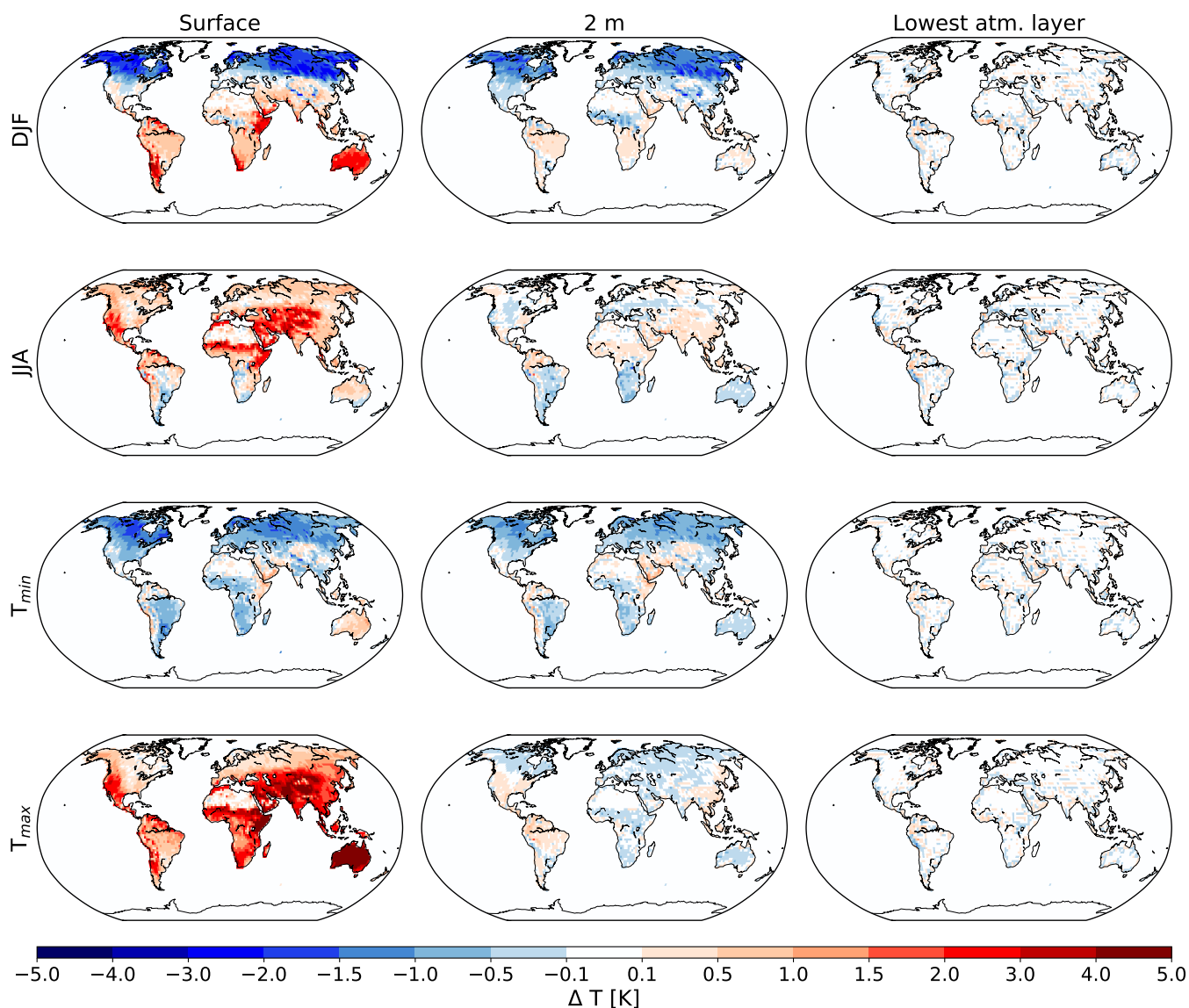
Figure 2. Seasonal and diurnal temperature response to the local effects of deforestation, separately for boreal winter (DJF) and summer (JJA), daily maximum (T_{max}) and minimum temperature (T_{min}).

atmospheric conditions may become neutral or stable near the surface (Fig. S2), and thus a different Monin-Obukhov function γ is employed in equation 2 (ECMWF Research Department, 1991), with the consequence that near-surface air temperature at deforested locations stays closer to surface temperature compared to daytime conditions (Figure S3 a).

3.2 Different temperature response of surface temperature and air temperature across climate models

While the above results refer only to the MPI-ESM climate model, the local effects on T_{surf} and T_{2m} also differ in other climate models (Fig. 3). We analyze the local effects of historical deforestation and the average over mid-latitude areas (40-60° N) that experienced intense deforestation ($\geq 15\%$) since 1860. We choose the northern mid-latitudes for two reasons: first,

5 this is where historically deforestation happened, and regions with intense deforestation are required in the moving-window approach for the isolation of the local effects across models (Methods), and second, it is interesting to analyze the local effects on temperature there because they have a different sign in the winter (DJF) and summer season (JJA)(Fig. 2).

In most models (with the exception of CanESM2 and GFDL-CM3), T_{surf} and T_{2m} respond similarly for changes in annual means in the mid-latitude areas (Fig. 3 a). This includes the MPI-ESM – the different spatial patterns of warming and cooling

10 for T_{surf} and T_{2m} discussed for the MPI-ESM in the previous chapter (Fig. 1 results in similar responses when averaged over mid-latitude areas (40-60° N) that experienced intense deforestation ($\geq 15\%$) since 1860. A difference in response between T_{surf} and T_{2m} becomes apparent also for the mid-latitudes, however, when not annual mean, but DJF and JJA seasons are considered separately. Almost all of the tested models show substantial differences between T_{surf} and T_{2m} at seasonal scale (Fig. 3 b-c).
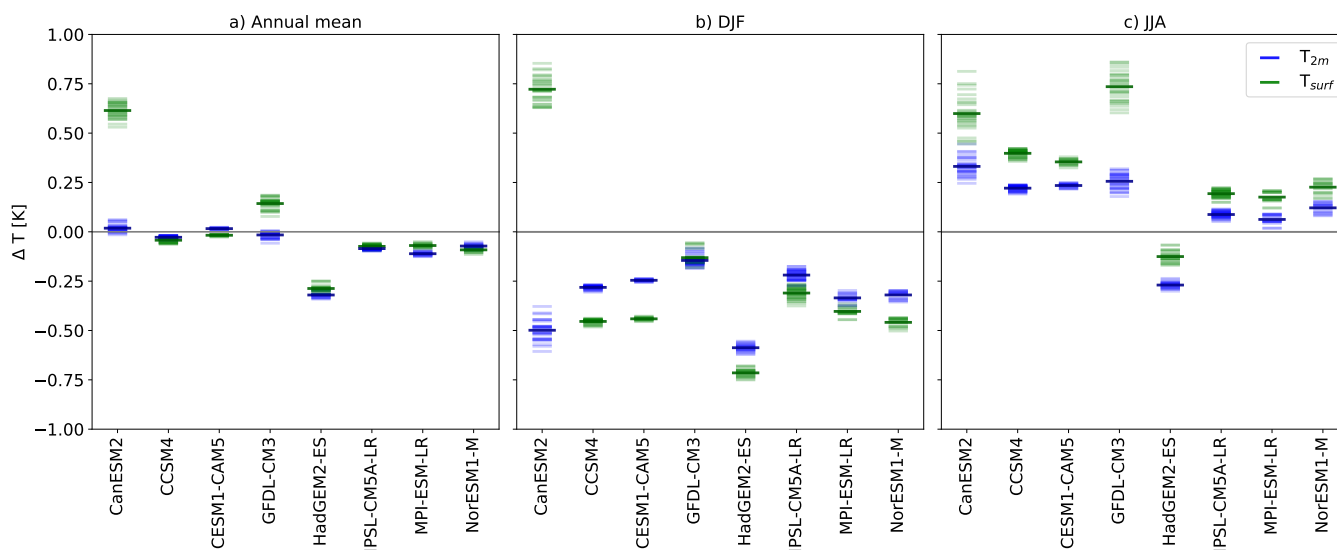
Figure 3. Local effects on near-surface air temperature (T_{2m}) and surface temperature (T_{surf}) for CMIP5 models. Values are averaged over mid-latitude areas (40-60° N) that experienced intense deforestation ($\geq 15\%$) since 1860. Positive values indicate a deforestation-induced warming. Each transparent marker denotes one combination of ensemble members from the 'historical' and 'piControl' experiments, respectively. The solid markers denote the mean values. The corresponding maps are shown in Figs. S4-S6. The local effects are isolated as in the study by Lejeune et al. (2018).

15 In JJA (Fig. 3c), all but one model show a surface warming locally, with the T_{surf} responding more strongly than T_{2m} by a factor of around two (Table S1). Only the HadGEM2-ES climate model is an outlier: there, T_{surf} responds to deforestation

Earth System
Dynamics
Discussions

with a local cooling (-0.13 K), which is not in agreement with observation-based studies (Li et al., 2015; Alkama and Cescatti, 2016; Bright et al., 2017; Duveiller et al., 2018), and in the HadGEM2-ES T_{2m} cools even more strongly (-0.27 K) than T_{surf}.

In DJF (Fig. 3b), all but one model show a surface cooling locally, again with T_{surf} responding stronger than T_{2m} in most models. An exception is the CanESM2 model, which locally responds to deforestation with a strong T_{surf} warming and T_{2m} cooling. In some of the other climate models (CCSM4, CESM1-CAM5, NorESM1-M), the T_{surf} cooling is approximately twice the cooling of T_{2m}, analogous to the JJA response. In other models (GFDL-CM3, HadGEM2-ES, IPSL-CM5A-LR, MPI-ESM-LR), the the two variables respond more similarly in DJF compared to JJA.

Overall, the inter-model comparison suggests that the different response of T_{surf} and T_{2m} is not specific to the MPI-ESM model. In agreement with previous studies (Pitman et al., 2009; Boisier et al., 2012; de Noblet-Ducoudré et al., 2012; Lejeune et al., 2017), the inter-model spread in the temperature response in Fig. 3 is large (e.g., in JJA inter-model (excluding the HadGEM2) standard deviation 0.20 K, inter-model mean 0.38 K). However, the investigated models agree better concerning the ratio between the T_{2m} and T_{surf} response (JJA inter-model (excluding the HadGEM2) standard deviation 0.11, inter-model mean 0.50). Both for DJF and JJA (Table S1), and for most of the investigated models, the ratio of changes in T_{2m} and T_{surf} of 0.5 is largely independent of the magnitude and sign of the surface temperature response. Assuming that deforestation does locally not affect T_{atm}, the temperature response of T_{2m} is between zero and the response of T_{surf} with a ratio that depends on the exact way in which T_{2m} is calculated in the respective models (but most likely all models use a Monin-Obukhov approach). Further studies may investigate the validity of the assumption that T_{atm} locally does not respond to deforestation, as well as to what extent the calculation of T_{2m} differs across models and how this influences the deforestation response.

4   Discussion and conclusions

This study shows that in climate models, surface temperature (T_{surf}) and near-surface air temperature (T_{2m}) respond differently to deforestation. In the MPI-ESM, the nonlocal response (present also in locations that were not deforested) of T_{surf} and T_{2m} is similar, while their local response (present only in locations that were deforested) differs. In the northern mid- and high latitudes, the annual mean local cooling of T_{2m} can be stronger than the local cooling of T_{surf}, but in most regions T_{surf} responds stronger than T_{2m}. Across most models, the local effects of deforestation on T_{surf} and T_{2m} in the mid-latitudes differ by a factor of two in both investigated seasons.

This study illustrates that the conclusions concerning the effects of deforestation can depend on the considered temperature measure. In observation-based studies, the magnitude and sign of deforestation effects can differ depending on the temperature measure; for instance, satellite–based studies on radiometric surface temperature (e.g., Li et al., 2015; Alkama and Cescatti, 2016; Duveiller et al., 2018) found that the local effects of deforestation turn from a cooling in the boreal regions to a warming further south at between 45-55°N (the latitudinally averaged local temperature effect at 50°N is about -0.5 K to 0.5 K, see Fig. 1 in the study by Winckler et al. (2018)). On the other hand, in-situ–based studies on T_{2m} found that the transition from

warming to cooling is located much further south, at around 35°N, and that deforestation at 50°N leads to a cooling of around -1 K (e.g., Lee et al., 2011; Zhang et al., 2014). These differences in magnitude and pattern between ΔT_{surf} and ΔT_{2m} largely agree with our findings (more cooling for T_{2m} than for T_{surf} in the mid-latitudes for the local effects in the MPI-ESM, see Fig. 1) and thus our results make it seem plausible that the consideration of different temperature measures can

5 explain some of the discrepancies between the satellite-based and in-situ–based studies. A consistent comparison between satellite–based and in-situ–based studies can be challenging because they may report different variables. Satellite-based data-sets usually reported changes in radiometric surface temperature, which is a combination of temperature of the top of the vegetation and the soil (through gaps in the canopy). Satellite-based direct estimates of air temperature (based on the intensity of upwelling microwave radiation from atmospheric oxygen) are available only for broad vertical layers of the atmosphere and

10 at coarse spatial scale (Von Engeln and Bühler, 2002). Instead of direct observations, air temperature was derived from surface temperature by empirical methods (Alkama and Cescatti, 2016) or process-oriented models (i.e. by solving the surface energy budget) (Hou et al., 2013). More direct observational investigations on the effects of deforestation on air temperature were based on recordings from weather stations and Fluxnet towers, which measure temperature at different heights. For instance, weather stations, e.g. in forest clearings, recorded temperatures at a height of between 1.2 and 2.0 m above ground level (WMO,

15 2008) while Fluxnet sites recorded temperatures typically 2-15 m above forest canopies (Lee et al., 2011; Zhang et al., 2014). The different measurement height may lead to systematic differences because of the steep vertical temperature profile that develops near the surface under stable atmospheric conditions (e.g. at night) especially over open land (Schultz et al., 2017). In contrast to satellite-based products, which are available at a high spatial resolution, the spatial distribution of Fluxnet towers and weather stations is biased toward developed countries and there is a relatively poor geographical coverage of rural areas

20 in developing countries where deforestation has occurred recently (Hansen et al., 2013). To perform a meaningful comparison, near-surface air temperature would have to be available at the same height above canopy top (preferably multiple heights) for the various land cover types and with a good geographical coverage.

The comparison of deforestation effects in observations and climate models is even more challenging. First, the respective variables in the models are only a proxy of the variables that were recorded in observation-based data-sets (see Methods for the

25 MPI-ESM). Second, model-based studies usually analyzed the combination of local and nonlocal effects, while observation-based studies only analyzed local effects, for which T_{surf} and T_{2m} respond differently (Fig. 2). Any nonlocal effects are excluded from the observations because possible nonlocal effects are present both in forest locations and nearby open land, and thus the nonlocal effects cancel out when looking at the difference between forests and open land, which is acknowledged by these studies (e.g., Li et al., 2015; Alkama and Cescatti, 2016; Bright et al., 2017; Duveiller et al., 2018). Note that Earth system

30 models consider further climate effects when simulating deforestation-induced releases of land carbon into the atmosphere (e.g., Pongratz et al., 2010; Le Quéré et al., 2017). Because CO_2 is a well-mixed greenhouse gas the resulting warming can be expected to act essentially nonlocally and likely influences influence surface and air temperature similarly.

The different temperature variables that are considered in studies about the deforestation effects are relevant for different questions and applications. Satellite-based studies on changes in radiometric surface temperature provided important informa-

35 tion about the biophysical mechanisms of surface energy partitioning and thereby surface-atmosphere interactions (Duveiller

**Earth System
Dynamics**
Discussions

et al., 2018), as well as habitat and vegetative function (De Frenne et al., 2013). Compared to changes in surface temperature, changes in air temperature may be considered more relevant for human living conditions because it matters for the perceived temperature (e.g., Staiger et al., 2011). Within- and below-canopy air temperature is the most relevant variable for organisms that live within the forests (e.g., De Frenne et al., 2013). However, there are little observations and few models can simulate

5   vertical within-canopy temperature profiles (e.g., Chen et al., 2016). Hence, we did not address within-canopy temperature in the current study.

The different response of surface temperature (T_{surf}) and air temperature (T_{2m}) is relevant for climate policies. Strategies that aim at adapting locally to warming air temperature may focus on perceived temperature and thus T_{2m}, but this study shows that the local effects on T_{2m} may substantially differ from those on T_{surf}, in particular for mean daily maximum

10 temperature (see Fig. 2). Consequently, strategies in the agricultural sector that aim at adapting locally to warming soil and canopy temperatures may focus on the local effects on surface temperature because this variable is relevant for the organisms that live there. On the other hand, for international policies that aim at mitigating global warming, what matters is not only temperature at the location of deforestation but also in nearby and in remote regions. Thus, international policies mainly additionally consider the nonlocal effects. For the nonlocal effects, the response of T_{surf} and T_{2m} are rather similar (Fig. 2)

15 and a distinction between the two temperature measures is therefore less relevant. To sum up, this study emphasizes that the local biogeophysical effects of deforestation influence T_{surf} and T_{2m} differently, and thus, a careful choice based on the respective application has to be made whether a study should focus on changes in surface temperature or near-surface air temperature.

Author contributions. J.W., C.H.R and J.P. designed the research; J.W. performed the simulations with the MPI-ESM, analyzed the data and

20 drafted the manuscript. All authors contributed to the interpretation of the data and revision of the manuscript.

Earth System
Dynamics
Discussions

References

Alkama, R. and Cescatti, A.: Biophysical climate impacts of recent changes in global forest cover, Science, 351, 600–604, https://doi.org/10.1126/science.aac8083, 2016.

Bala, G., Caldeira, K., Wickett, M., Phillips, T. J., Lobell, D. B., Delire, C., and Mirin, A.: Combined climate and carbon-cycle effects of
5   large-scale deforestation, Proceedings of the National Academy of Sciences, 104, 6550–6555, https://doi.org/10.1073/pnas.0608998104, 2007.

Bathiany, S., Claussen, M., Brovkin, V., Raddatz, T., and Gayler, V.: Combined biogeophysical and biogeochemical effects of large-scale forest cover changes in the MPI Earth system model, Biogeosciences, 7, 1383–1399, https://doi.org/10.5194/bg-7-1383-2010, 2010.

Boisier, J. P., de Noblet-Ducoudré, N., Pitman, A. J., Cruz, F. T., Delire, C., van den Hurk, B. J. J. M., van der Molen, M. K.,
10   Müller, C., and Voldoire, A.: Attributing the impacts of land-cover changes in temperate regions on surface temperature and heat fluxes to specific causes: Results from the first LUCID set of simulations, Journal of Geophysical Research: Atmospheres, 117, 1–16, https://doi.org/10.1029/2011JD017106, 2012.

Bonan, G. B.: Forests and climate change: forcings, feedbacks, and the climate benefits of forests., Science, 320, 1444–1449, https://doi.org/10.1126/science.1155121, 2008.

15   Bright, R. M., Davin, E. L., O'Halloran, T. L., Pongratz, J., Zhao, K., and Cescatti, A.: Local temperature response to land cover and management change driven by non-radiative processes, Nature Climate Change, 7, 296–302, https://doi.org/10.1038/nclimate3250, 2017.

Campbell, G. S. and Norman, J. M.: An Introduction to Environmental Biophysics, Springer-Verlag New York, https://doi.org/10.1007/978-1-4612-1626-1, 1998.

Chen, J., Saunders, S. C., Crow, T. R., Naiman, R. J., Brosofske, K. D., Mroz, G. D., Brookshire, B. L., and Franklin, J. F.: Microclimate in
20   Forest Ecosystem and Landscape Ecology, BioScience, 49, 288–297, 1999.

Chen, Y., Ryder, J., Bastrikov, V., McGrath, M. J., Naudts, K., Otto, J., Ottlé, C., Peylin, P., Polcher, J., Valade, A., Black, A., Elbers, J. A., Moors, E., Foken, T., Van Gorsel, E., Haverd, V., Heinesch, B., Tiedemann, F., Knohl, A., Launiainen, S., Loustau, D., Ogeé, J., Vessala, T., and Luyssaert, S.: Evaluating the performance of land surface model ORCHIDEE-CAN v1.0 on water and energy flux estimation with a single-and multi-layer energy budget scheme, Geoscientific Model Development, 9, 2951–2972, https://doi.org/10.5194/gmd-9-2951-
25   2016, 2016.

Claussen, M., Brovkin, V., and Ganopolski, A.: Biogeophysical versus biogeochemical feedbacks of large-scale land cover change, Geophysical Research Letters, 28, 1011–1014, 2001.

Davin, E. L. and de Noblet-Ducoudre, N.: Climatic impact of global-scale deforestation: radiative versus nonradiative processes, Journal of Climate, 23, 97–112, https://doi.org/10.1175/2009JCLI3102.1, 2010.

30   De Frenne, P., Rodriguez-Sanchez, F., Coomes, D. A., Baeten, L., Verstraeten, G., Vellend, M., Bernhardt-Romermann, M., Brown, C. D., Brunet, J., Cornelis, J., Decocq, G. M., Dierschke, H., Eriksson, O., Gilliam, F. S., Hedl, R., Heinken, T., Hermy, M., Hommel, P., Jenkins, M. A., Kelly, D. L., Kirby, K. J., Mitchell, F. J. G., Naaf, T., Newman, M., Peterken, G., Petrik, P., Schultz, J., Sonnier, G., Van Calster, H., Waller, D. M., Walther, G.-R., White, P. S., Woods, K. D., Wulf, M., Graae, B. J., and Verheyen, K.: Micro-climate moderates plant responses to macroclimate warming, Proceedings of the National Academy of Sciences, 110, 18 561–18 565,
35   https://doi.org/10.1073/pnas.1311190110, 2013.

de Noblet-Ducoudré, N., Boisier, J.-P., Pitman, A., Bonan, G. B., Brovkin, V., Cruz, F., Delire, C., Gayler, V., van den Hurk, B. J. J. M., Lawrence, P. J., van der Molen, M. K., Müller, C., Reick, C. H., Strengers, B. J., and Voldoire, A.: Determining robust impacts of land-

use-induced land cover changes on surface climate over North America and Eurasia: Results from the first set of LUCID experiments, Journal of Climate, 25, 3261–3281, https://doi.org/10.1175/JCLI-D-11-00338.1, 2012.

Deser, C., Knutti, R., Solomon, S., and Phillips, A. S.: Communication of the role of natural variability in future North American climate, Nature Climate Change, 2, 775–779, https://doi.org/10.1038/nclimate1562, 2012.

5 Devaraju, N., Bala, G., and Modak, A.: Effects of large-scale deforestation on precipitation in the monsoon regions: Remote versus local effects, Proceedings of the National Academy of Sciences, 112, 3257–3262, https://doi.org/10.1073/pnas.1423439112, 2015.

Duveiller, G., Hooker, J., and Cescatti, A.: The mark of vegetation change on Earth's surface energy balance, Nature Communications, 9, 1–12, https://doi.org/10.1038/s41467-017-02810-8, 2018.

ECMWF Research Department: Research Manual 3, ECMWF forecast model, Physical parametrization, 3rd Edition, 1991.

10 Findell, K. L., Knutson, T. R., and Milly, P. C. D.: Weak simulated extratropical responses to complete tropical deforestation, Journal of Climate, 19, 2835–2850, https://doi.org/10.1175/JCLI3737.1, 2006.

Gibbard, S., Caldeira, K., Bala, G., Phillips, T. J., and Wickett, M.: Climate effects of global land cover change, Geophysical Research Letters, 32, 1–4, https://doi.org/10.1029/2005GL024550, 2005.

Giorgetta, M. A., Roeckner, E., Mauritsen, T., Bader, J., Crueger, T., Esch, M., Rast, S., Kornblueh, L., Schmidt, H., Kinne, S., Hohenegger,
15 C., Möbis, B., Krismer, T., Wieners, K.-H., and Stevens, B.: The atmospheric general circulation model ECHAM6 - Model description, Tech. Rep. 135, Max-Planck-Institute for Meteorology, Hamburg, 2013.

Hansen, M. C., Potapov, P. V., Moore, R., Hancher, M., Turubanova, S. a., and Tyukavina, A.: High-resolution global maps of 21st-century forest cover change, Science, 342, 850–853, https://doi.org/10.1126/science.1244693, 2013.

Hou, P., Chen, Y., Qiao, W., Cao, G., Jiang, W., and Li, J.: Near-surface air temperature retrieval from satellite images and influence by
20 wetlands in urban region, Theoretical and Applied Climatology, 111, 109–118, https://doi.org/10.1007/s00704-012-0629-7, 2013.

Jin, M. and Dickinson, R. E.: Land surface skin temperature climatology: Benefitting from the strengths of satellite observations, Environmental Research Letters, 5, https://doi.org/10.1088/1748-9326/5/4/044004, 2010.

Jones, A. D., Collins, W. D., and Torn, M. S.: On the additivity of radiative forcing between land use change and greenhouse gases, Geophysical Research Letters, 40, 4036–4041, https://doi.org/10.1002/grl.50754, 2013.

25 Lague, M. and Swann, A.: Progressive Midlatitude Afforestation: Impacts on Clouds, Global Energy Transport, and Precipitation, Journal of Climate, 29, 5561–5573, https://doi.org/10.1175/JCLI-D-15-0748.1, 2016.

Le Quéré, C., Andrew, R. M., Friedlingstein, P., Sitch, S., Pongratz, J., Manning, A. C., Ivar Korsbakken, J., Peters, G. P., Canadell, J. G., Jackson, R. B., Boden, T. A., Tans, P. P., Andrews, O. D., Arora, V. K., Bakker, D. C., Barbero, L., Becker, M., Betts, R. A., Bopp, L., Chevallier, F., Chini, L. P., Ciais, P., Cosca, C. E., Cross, J., Currie, K., Gasser, T., Harris, I., Hauck, J., Haverd, V., Houghton, R. A., Hunt,
30 C. W., Hurtt, G., Ilyina, T., Jain, A. K., Kato, E., Kautz, M., Keeling, R. F., Klein Goldewijk, K., Körtzinger, A., Landschützer, P., Lefèvre, N., Lenton, A., Lienert, S., Lima, I., Lombardozzi, D., Metzl, N., Millero, F., Monteiro, P. M., Munro, D. R., Nabel, J. E., Nakaoka, S. I., Nojiri, Y., Antonio Padin, X., Peregon, A., Pfeil, B., Pierrot, D., Poulter, B., Rehder, G., Reimer, J., Rödenbeck, C., Schwinger, J., Séférian, R., Skjelvan, I., Stocker, B. D., Tian, H., Tilbrook, B., Tubiello, F. N., Laan-Luijkx, I. T., Werf, G. R., Van Heuven, S., Viovy, N., Vuichard, N., Walker, A. P., Watson, A. J., Wiltshire, A. J., Zaehle, S., and Zhu, D.: Global Carbon Budget 2017, Earth System Science
35 Data, 10, 405–448, https://doi.org/10.5194/essd-10-405-2018, 2017.

Leclerc, M. and Foken, T.: Footprints in Micrometeorology and Ecology, Springer Berlin Heidelberg, https://doi.org/10.1007/978-3-642-54545-0, 2014.

Lee, X., Goulden, M. L., Hollinger, D. Y., Barr, A., Black, T. A., Bohrer, G., Bracho, R., Drake, B., Goldstein, A., Gu, L., Katul, G., Kolb, T., Law, B. E., Margolis, H., Meyers, T., Monson, R., Munger, W., Oren, R., Paw U, K. T., Richardson, A. D., Schmid, H. P., Staebler, R., Wofsy, S., and Zhao, L.: Observed increase in local cooling effect of deforestation at higher latitudes, Nature, 479, 384–387, https://doi.org/10.1038/nature10588, 2011.

5   Lejeune, Q., Seneviratne, S. I., and Davin, E. L.: Historical land-cover change impacts on climate: Comparative assessment of LUCID and CMIP5 multimodel experiments, Journal of Climate, 30, 1439–1459, https://doi.org/10.1175/JCLI-D-16-0213.1, 2017.

Lejeune, Q., Davin, E. L., Gudmundsson, L., Winckler, J., and Seneviratne, S. I.: Historical deforestation increased the risk of heat extremes in northern mid-latitudes, Nature Climate Change, 8, 386–390, https://doi.org/10.1038/s41558-018-0131-z, 2018.

Li, Y., Zhao, M., Motesharrei, S., Mu, Q., Kalnay, E., and Li, S.: Local cooling and warming effects of forests based on satellite observations.,
10   Nature Communications, 6, 1–8, https://doi.org/10.1038/ncomms7603, 2015.

Li, Y., de Noblet-Ducoudré, N., Davin, E. L., Zeng, N., Motesharrei, S., Li, S. C., and Kalnay, E.: The role of spatial scale and background climate in the latitudinal temperature response to deforestation, Earth System Dynamics Discussions, 7, 167–181, https://doi.org/10.5194/esdd-6-1897-2015, 2016.

Luyssaert, S., Schulze, E.-D., Börner, A., Knohl, A., Hessenmöller, D., Law, B. E., Ciais, P., and Grace, J.: Old-growth forests as global
15   carbon sinks., Nature, 455, 213–215, https://doi.org/10.1038/nature07276, 2008.

Pitman, A. J., de Noblet-Ducoudré, N., Cruz, F. T., Davin, E. L., Bonan, G. B., Brovkin, V., Claussen, M., Delire, C., Ganzeveld, L., Gayler, V., van den Hurk, B. J. J. M., Lawrence, P. J., van der Molen, M. K., Müller, C., Reick, C. H., Seneviratne, S. I., Strengers, B. J., and Voldoire, A.: Uncertainties in climate responses to past land cover change: First results from the LUCID intercomparison study, Geophysical Research Letters, 36, 1–6, https://doi.org/10.1029/2009GL039076, 2009.

20   Pongratz, J., Reick, C. H., Raddatz, T., and Claussen, M.: A reconstruction of global agricultural areas and land cover for the last millennium, Global Biogeochemical Cycles, 22, 1–16, https://doi.org/10.1029/2007GB003153, 2008.

Pongratz, J., Reick, C. H., Raddatz, T., and Claussen, M.: Biogeophysical versus biogeochemical climate response to historical anthropogenic land cover change, Geophys. Res. Lett., 37, 1–5, https://doi.org/10.1029/2010GL043010, 2010.

Ramankutty, N. and Foley, J. A.: Estimating historical changes in global land cover: Croplands from 1700 to 1992, Global Biogeochemical
25   Cycles, 13, 997–1027, 1999.

Schultz, N. M., Lawrence, P. J., and Lee, X.: Global satellite data highlights the diurnal asymmetry of the surface temperature response to deforestation, Journal of Geophysical Research: Biogeosciences, 122, 903–917, https://doi.org/10.1002/2016JG003653, 2017.

Staiger, H., Laschewski, G., and Graetz, A.: The perceived temperature – a versatile index for the assessment of the human thermal environment. Part A: Scientific basics, International Journal of Biometeorology, 56, 165–176, https://doi.org/10.1007/s00484-011-0409-6,
30   2011.

Stevens, B., Giorgetta, M., Esch, M., Mauritsen, T., Crueger, T., Rast, S., Salzmann, M., Schmidt, H., Bader, J., Block, K., Brokopf, R., Fast, I., Kinne, S., Kornblueh, L., Lohmann, U., Pincus, R., Reichler, T., and Roeckner, E.: Atmospheric component of the MPI-M Earth System Model: ECHAM6, Journal of Advances in Modeling Earth Systems, 5, 146–172, https://doi.org/10.1002/jame.20015, 2013.

Swann, A. L. S., Fung, I. Y., and Chiang, J. C. H.: Mid-latitude afforestation shifts general circulation and tropical precipitation, Proceedings
35   of the National Academy of Sciences, 109, 712–716, https://doi.org/10.1073/pnas.1116706108, 2012.

Taylor, K. E., Stouffer, R. J., and Meehl, G. A.: An Overview of CMIP5 and the Experiment Design, Bulletin of the American Meteorological Society, pp. 485–498, https://doi.org/10.1175/BAMS-D-11-00094.1, 2012.

UNFCCC: The Cancun Agreements: Land use, land-use change and forestry in Report of the Conference of the Parties serving as the meeting of the Parties to the Kyoto Protocol on its sixth session, pp. 1–32, 2011.

Vanden Broucke, S., Luyssaert, S., Davin, E. L., Janssens, I., Lipzig, N., Broucke, S. V., Luyssaert, S., Davin, E. L., Janssens, I., and Lipzig, N.: New insights in the capability of climate models to simulate the impact of LUC based on temperature decomposition of paired site observations, Journal of Geophysical Research: Atmospheres, 120, 1–20, https://doi.org/10.1002/2015JD023095, 2015.

Von Engeln, A. and Bühler, S.: Temperature profile determination from microwave oxygen emissions in limb sounding geometry, Journal of Geophysical Research Atmospheres, 107, 1–15, https://doi.org/10.1029/2001JD001029, 2002.

Winckler, J., Reick, C. H., and Pongratz, J.: Robust identification of local biogeophysical effects of land-cover change in a global climate model, Journal of Climate, 30, 1159–1176, https://doi.org/10.1175/JCLI-D-16-0067.1, 2017.

Winckler, J., Reick, C. H., Lejeune, Q., and Pongratz, J.: Nonlocal effects dominate the global mean surface temperature response to the biogeophysical effects of deforestation (submitted), submitted, 2018.

WMO: Guide to Meteorological Instruments and Methods of observation, vol. I & II, 2008.

Zhang, M., Lee, X., Yu, G., Han, S., Wang, H., Yan, J., Zhang, Y., Li, Y., Ohta, T., Hirano, T., Kim, J., Yoshifuji, N., and Wang, W.: Response of surface air temperature to small-scale land clearing across latitudes, Environmental Research Letters, 9, 7, https://doi.org/10.1088/1748-9326/9/3/034002, 2014.